

Supplementary Materials for
An injury-responsive *mmp14b* enhancer is required for heart regeneration

Ivana Zlatanova *et al.*

Corresponding author: Brian L. Black, brian.black@ucsf.edu

Sci. Adv. 9, eadh5313 (2023)
DOI: 10.1126/sciadv.adh5313

The PDF file includes:

Figs. S1 to S10
Tables S1 and S2
Legend for data S1

Other Supplementary Material for this manuscript includes the following:

Data S1

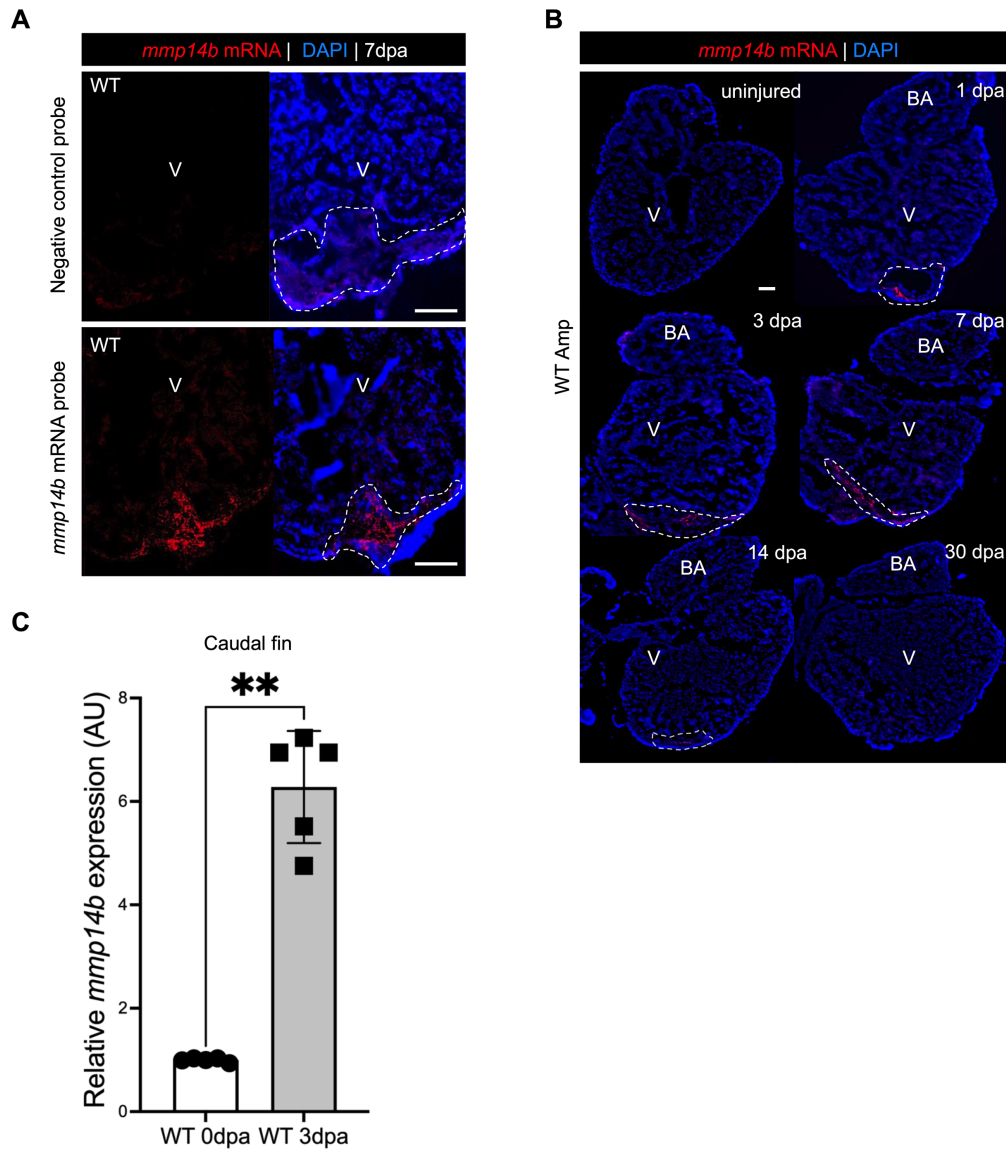


Fig. S1. *mmp14b* transcript expression during heart regeneration. (A) RNAscope *in situ* hybridization on sections of wild type zebrafish hearts at 7 dpa using an *mmp14b*-specific probe and negative control probe. (B) RNA-scope *in situ* hybridization for *mmp14b* expression in wild type zebrafish hearts at 1, 3, 7, 14, and 30 dpa. 6–8 sections from 6 hearts were analyzed. (C) Relative expression of *mmp14b* in wild type zebrafish caudal fin without injury and injured at 3 dpa as measured by RT-qPCR. Scale bars, 100 μ m (A and B) Statistical significance was determined using student's t-test. **, $p < 0.01$.

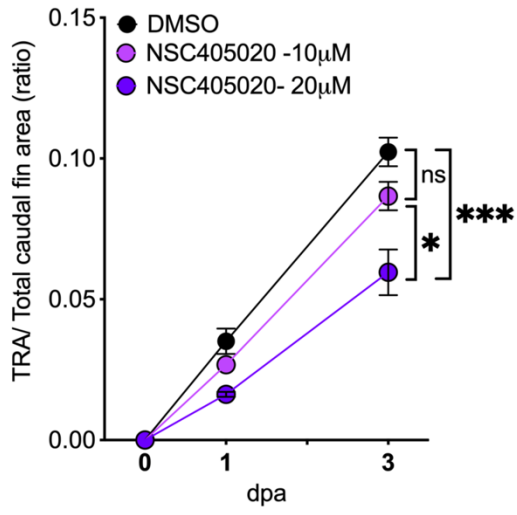
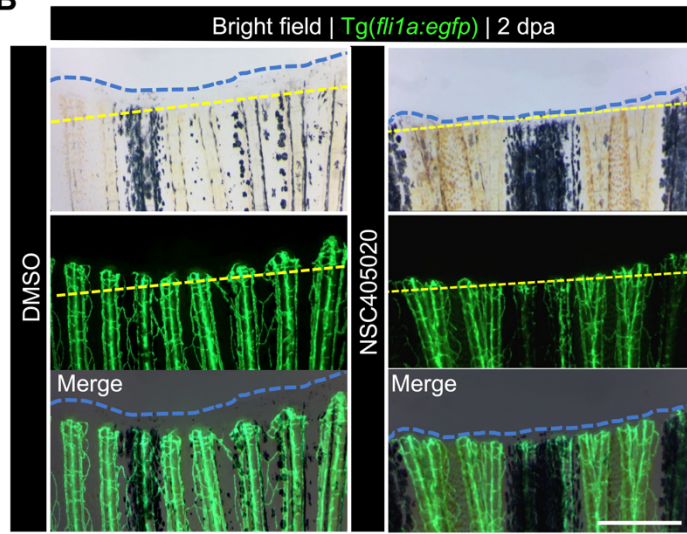
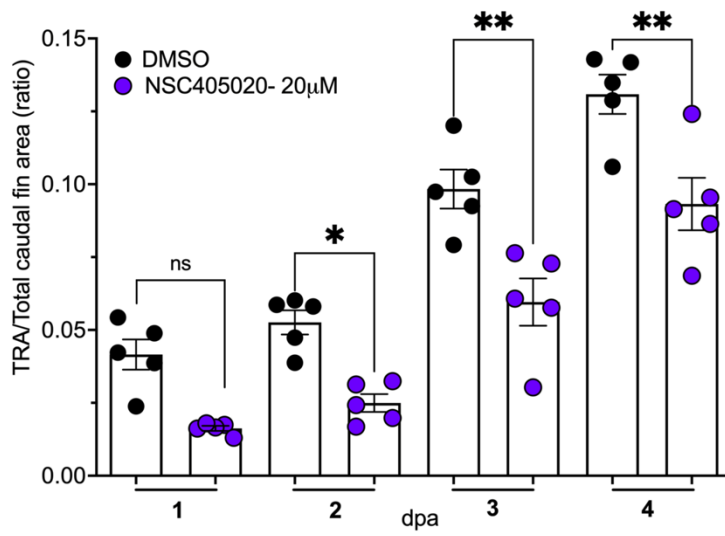
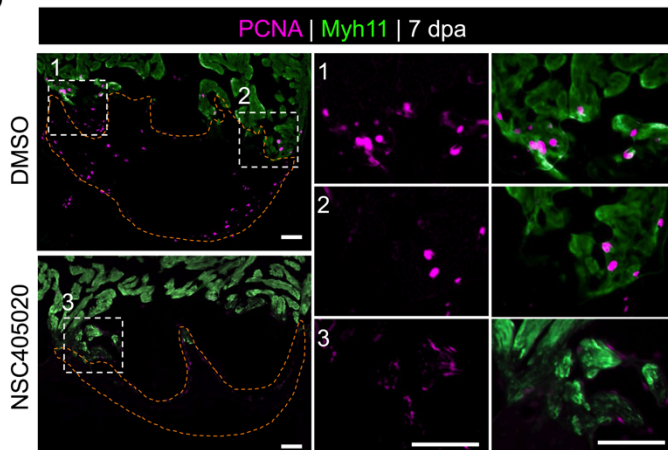
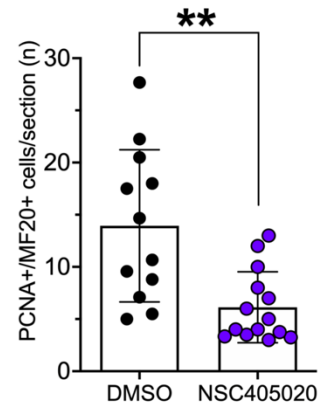
A**B****C****D****E**

Fig. S2. Pharmacologic inhibition of Mmp14b function impairs regeneration in zebrafish.

(A) Assessment of two concentrations of the MMMP-14 inhibitor NSC405020 on caudal fin regeneration. Tissue regeneration was significantly inhibited at 3 dpa in the presence of 20 μ M but not in the presence of 10 μ M NSC405020 when compared to DMSO; n=5-8 fish per group. (B) Representative bright field and fluorescent images of Tg(*fli1a:egfp*) zebrafish subjected to caudal fin amputation and either DMSO or 20 μ M NSC405020 at 2 dpa. Dashed blue lines approximate the blastema progression; dashed yellow lines represent the injury site. Note the inhibition of vessel growth and blastema progression in the presence of NSC405020 compared to DMSO. (C) Quantitative assessment of the total regenerated area (TRA) following caudal fin amputation in wild type zebrafish at 1, 2, 3, and 4 dpa in the presence of DMSO and 20 μ M NSC405020. (D) Heart sections from DMSO- and NSC405020-treated zebrafish subjected to ventricular amputation. Heart sections at 7 dpa stained by immunofluorescence for cardiomyocytes (α -Myh11/MF20 antibody; green) and cycling cells (α -PCNA antibody; magenta). Boxed regions are enlarged in (1-3). (E) Cardiomyocyte proliferation indices at 7 dpa in DMSO- and NSC405020-treated hearts. Scale bar: in (B) 400 μ m; in (D) 50 μ m. Statistical significance in (A and C) was determined using one- way ANOVA with Tukey's multiple comparisons test, in (E) was determined using student's t- test. ns, not significant; *, p<0.05; **, p<0.01; ***, p<0.001.

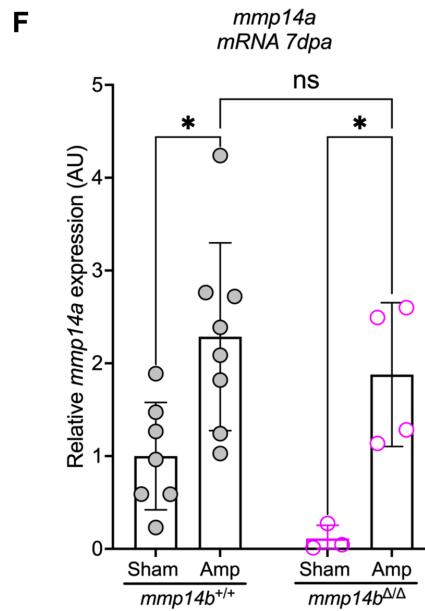
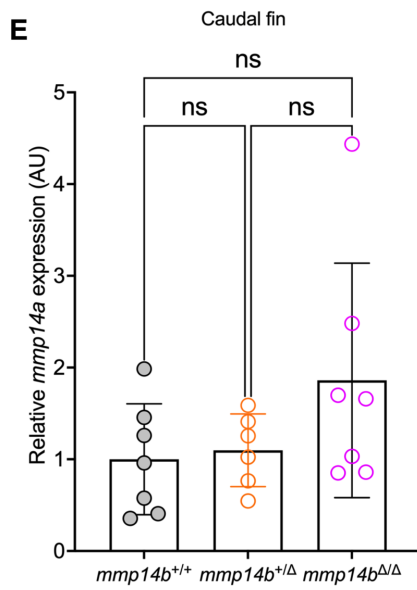
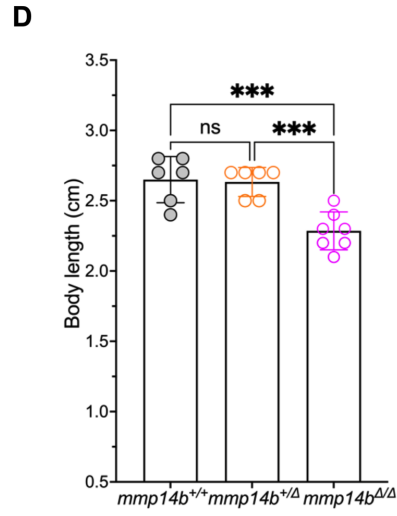
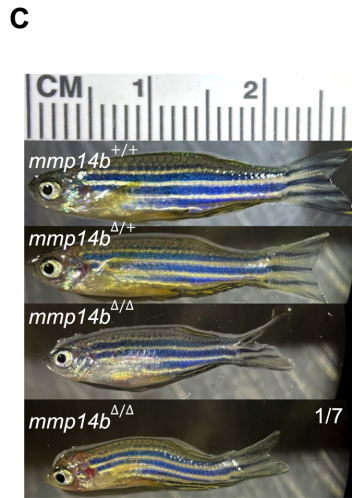
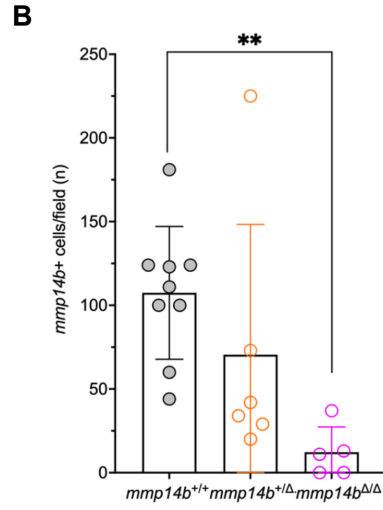
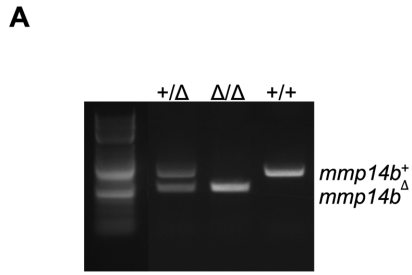


Fig. S3. Genetic inactivation of Mmp14b function in zebrafish. (A) PCR genotyping of a homozygous *mmp14b^{Δ/Δ}* mutant. (B) The number of *mmp14b*-positive cells in the heart is reduced in *mmp14b^{+/Δ}* and *mmp14b^{Δ/Δ}* compared to wild type *mmp14b^{+/+}* hearts at 7 dpa. (C) Representative images of *mmp14b^{+/+}*, *mmp14b^{+/Δ}*, and *mmp14b^{Δ/Δ}* zebrafish at 3 months age. The majority of *mmp14b^{Δ/Δ}* zebrafish are phenotypically normal, albeit shorter. Rarely (1/7), *mmp14b^{Δ/Δ}* zebrafish exhibit an evident skeletal phenotype (bottom panel). (D) The total body length of *mmp14b^{Δ/Δ}* zebrafish is significantly shorter than *mmp14b^{+/+}* and *mmp14b^{+/Δ}* zebrafish at 3 months. (E) Relative expression of *mmp14a* in *mmp14b^{+/+}*, *mmp14b^{+/Δ}* and *mmp14b^{Δ/Δ}* zebrafish caudal fin without injury as measured by RT-qPCR. (F) Relative expression of *mmp14a* in *mmp14b^{+/+}* and *mmp14b^{Δ/Δ}* zebrafish hearts without injury (Sham) and injured (Amp) at 7 dpa as measured by RT-qPCR. Statistical significance was determined using one-way ANOVA with Tukey's multiple comparisons test. ns, not significant; *, p<0.05; **, p<0.01; ***, p<0.001.

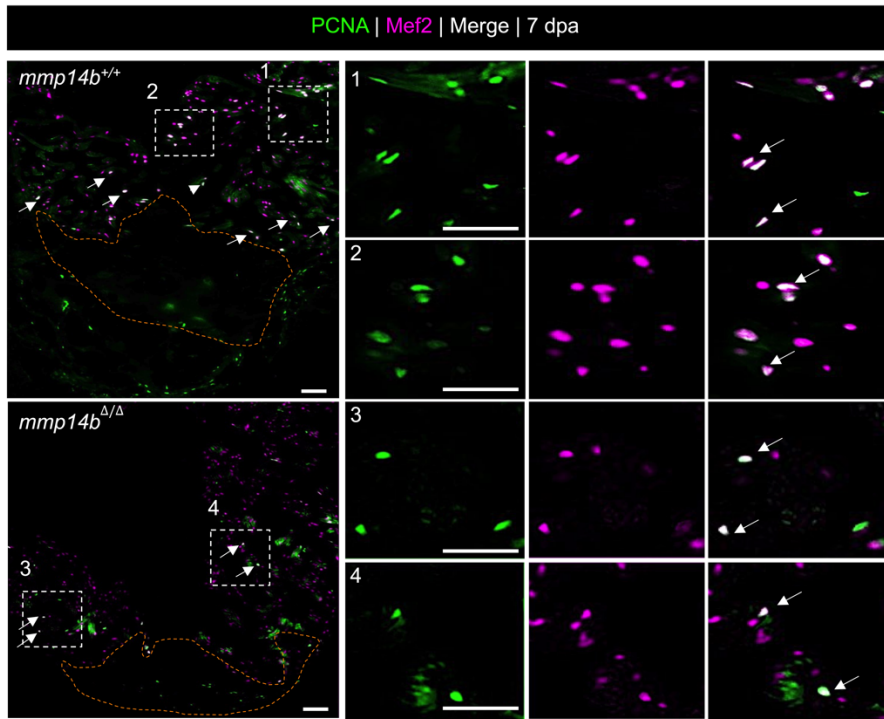
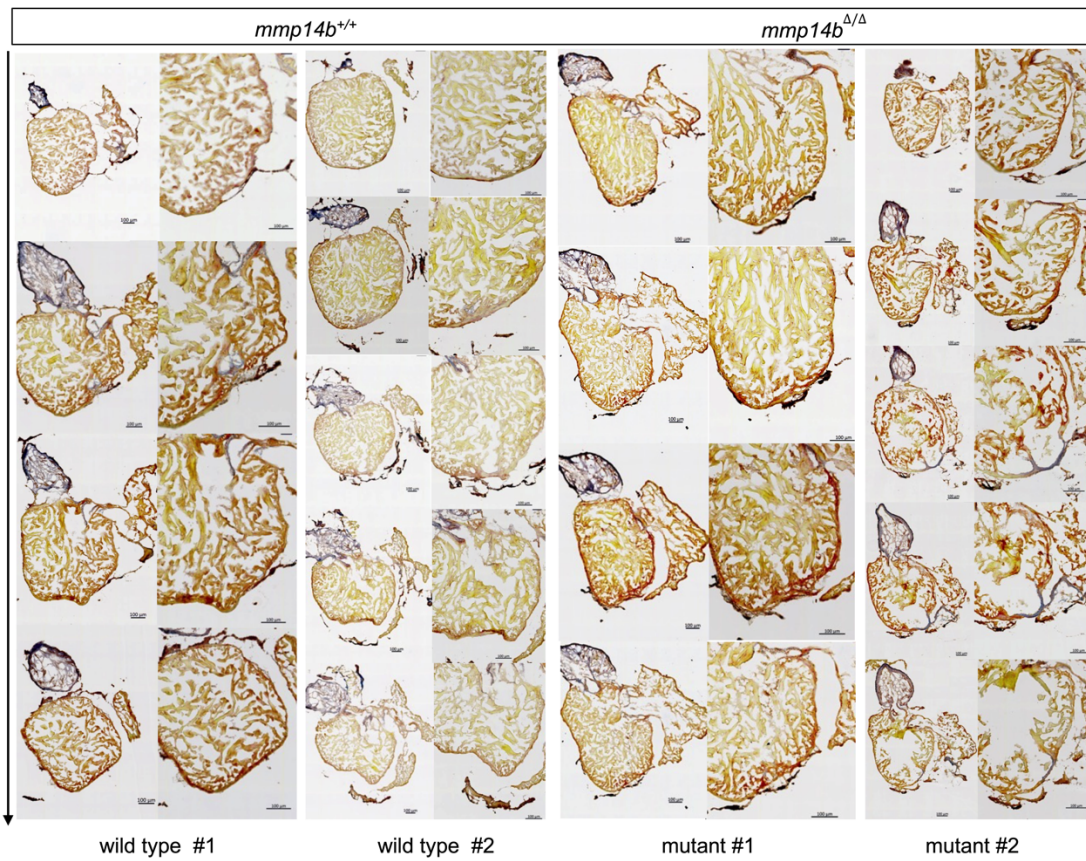
A**B**

Fig. S4. Genetic inactivation of *mmp14b* inhibits cardiomyocyte proliferation and scar resolution in adult zebrafish. (A) Heart sections of *mmp14b*^{+/+} and *mmp14b*^{Δ/Δ} hearts 7 dpa stained for cardiomyocyte nuclei (α-Mef2 antibody; magenta) and cycling cells (α-PCNA antibody; green). Boxed regions are enlarged in (1-4). Arrows highlight PCNA/Mef2 double-positive cardiomyocytes. Scale bars, 50 μm. (B) Frontal sections of adult *mmp14b*^{+/+} and *mmp14b*^{Δ/Δ} zebrafish hearts collected at 30 dpa and stained with AFOG to detect muscle (brown), fibrin (red), and collagen (blue). Two wild type *mmp14b*^{+/+} and two mutant *mmp14b*^{Δ/Δ} hearts with 4-5 sections per heart shown. Higher magnification images are shown in the right columns for each individual. The *mmp14b*^{+/+} and *mmp14b*^{Δ/Δ} sections shown in Fig. 2E are distinct sections belonging to the same series as wild type #1 and mutant #1, respectively.

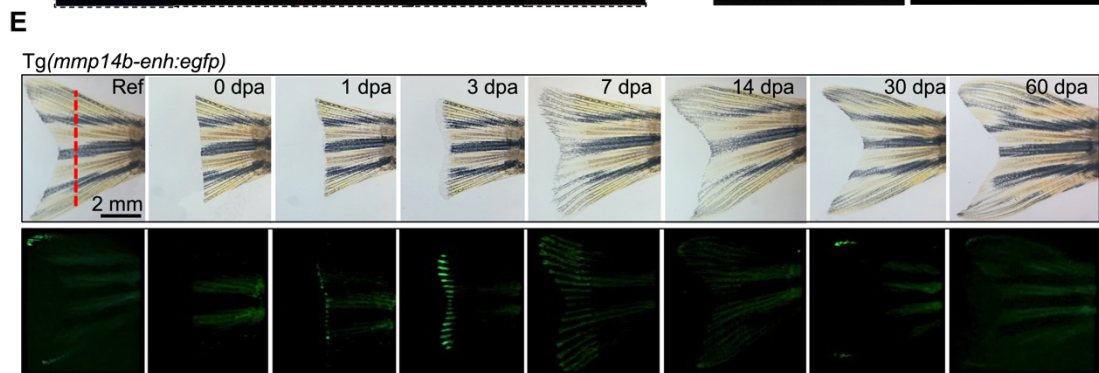
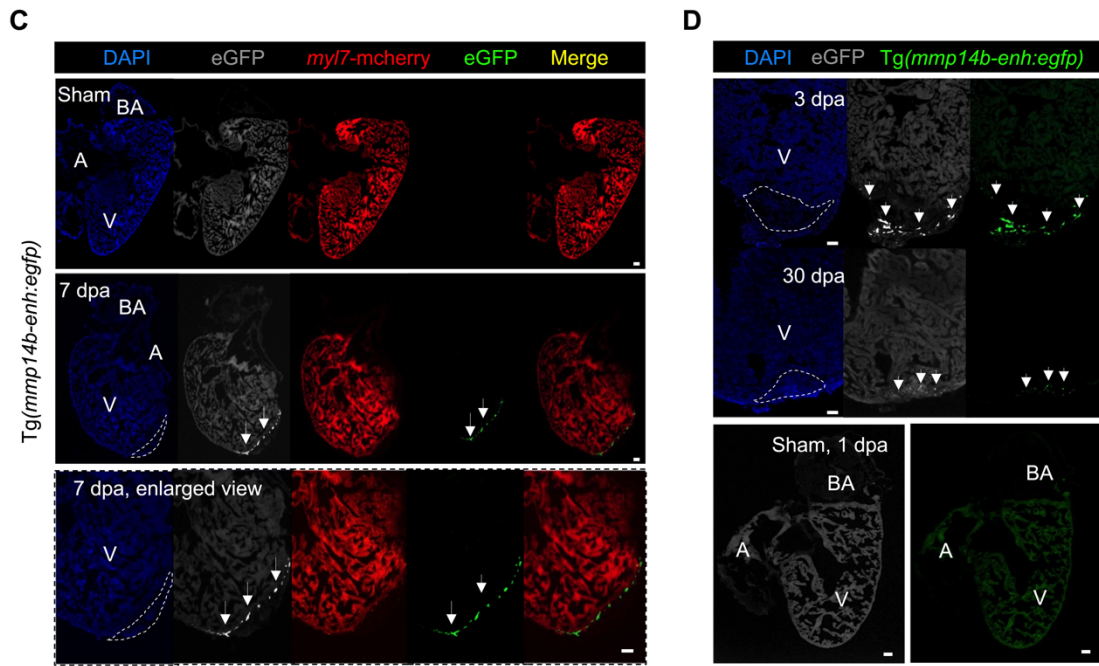
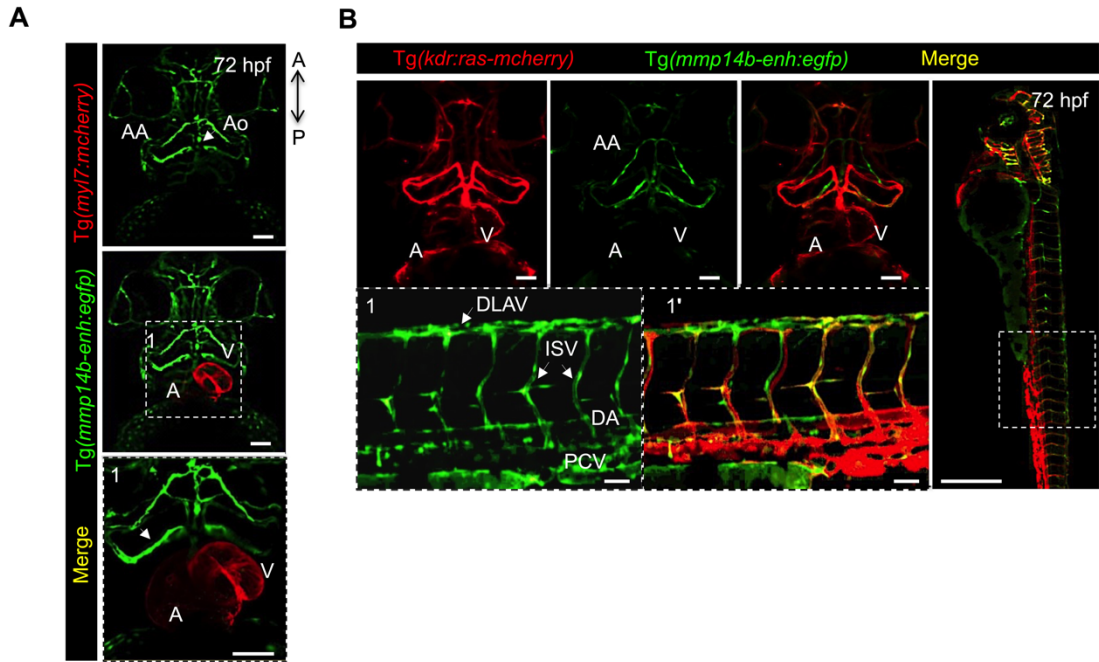


Fig. S5. *mmp14b-enh* is activated in endothelial cells during development and in response to injury. (A and B) Representative fluorescent images of zebrafish embryos at 72 hpf show endothelial-specific eGFP expression in Tg(*mmp14b-enh:egfp*) zebrafish. (A) Tg(*myl7:mCherry*) expression marks cardiomyocytes in red. Merged images are shown in the lower panels, and the boxed region is enlarged in (1). Note the absence of expression in the endocardium. (B) Tg(*kdrl:ras-mCherry*) expression marks the vascular endothelium. A stable *mmp14b-enh:egfp* transgenic zebrafish line demonstrates endothelial-specific expression. Whole-mount views of the zebrafish embryo. The boxed region is enlarged and rotated in (1, 1'). (C and D) Representative fluorescent images frontal sections of adult Tg(*mmp14b-enh:egfp*) hearts at 7dpa (c) and at 3 and 30 dpa (D), showing eGFP (green), cardiomyocytes (mCherry, red), and nuclei (DAPI, blue). No detectable eGFP fluorescence was observed in sham-operated hearts. Minimal eGFP activity was observed at 30 dpa (D). Dashed lines mark the approximate injured/regenerated area. Arrows mark eGFP+ cells at the injured/regenerated area. (E) Representative bright field (upper) and fluorescent (lower) images of caudal fin regeneration in Tg(*mmp14b-enh:egfp*) zebrafish from 0-60 dpa. The dashed red line approximates the amputation plane. A, atrium; AA, aortic arches; Ao; aorta; CV, cardinal vein; DA, dorsal aorta; DLAV; dorsal longitudinal anastomotic vessel; ISV, intersegmental vessels; PCV, posterior cardinal vein; V, ventricle. Scale bars, 50 μ m, except where indicated.

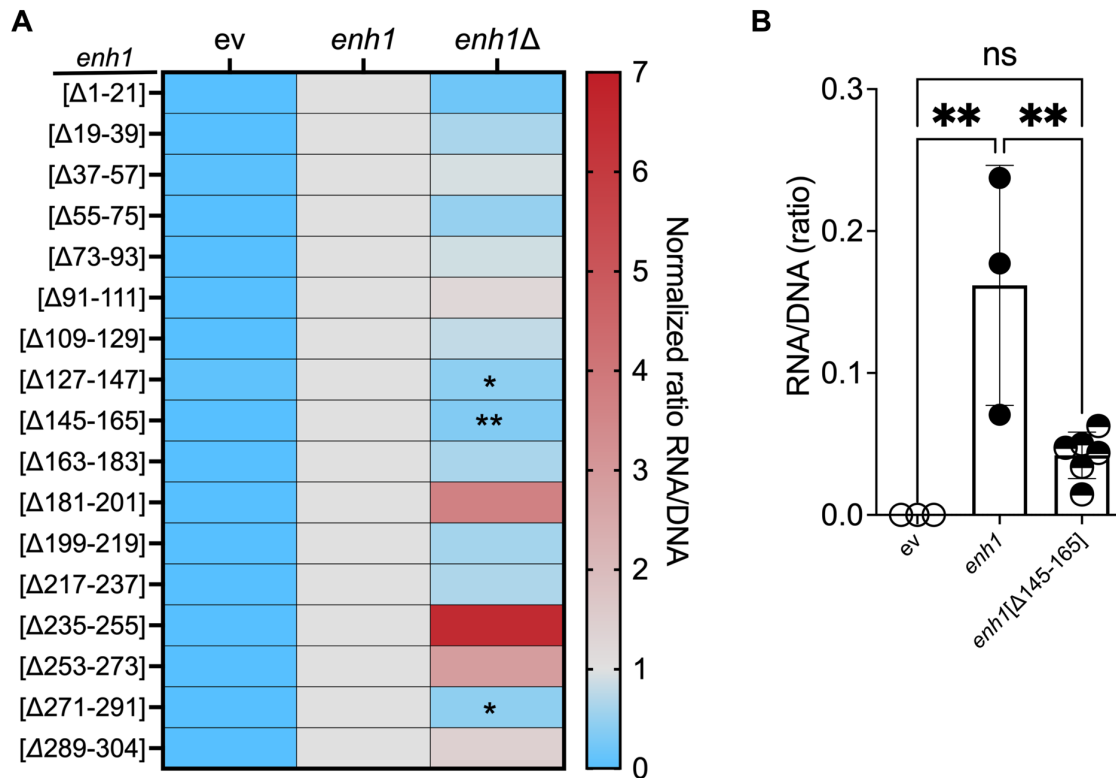


Fig. S6. Unbiased screen for *cis*-acting elements in *mmp14b-enh1* identifies a 21-bp region encompassing a functional TEAD binding site required for enhancer function *in vivo*. (A) Heat map depicting relative expression of reporter mRNA from each of 17 overlapping, 21-bp *mmp14b-enh1* deletions. Three deletions ($\Delta 127-147$, $\Delta 145-165$, and $\Delta 271-291$) displayed significant ($p < 0.05$) reduction in activity in transient transgenic analyses when compared to full length *mmp14b-enh1* (*enh1*, positive control). The empty *elb-egfp(tag)* vector (ev) negative control is also shown. In particular, *mmp14b-enh1*[$\Delta 145-165$] exhibited the largest and most significant reduction in expression in zebrafish larvae at 72 hpf. (B) RT-qPCR analysis for reporter mRNA expression directed by the empty vector (ev) transgene plasmid, *mmp14b-enh1* (*enh1*), and *mmp14b-enh1*[$\Delta 145-165$] showed significantly decreased expression of *enh1*[$\Delta 145-165$] compared to *enh1*. Statistical significance was determined using one-way ANOVA with Tukey's multiple comparisons test. ns, not significant; *, $p < 0.05$; **, $p < 0.01$.

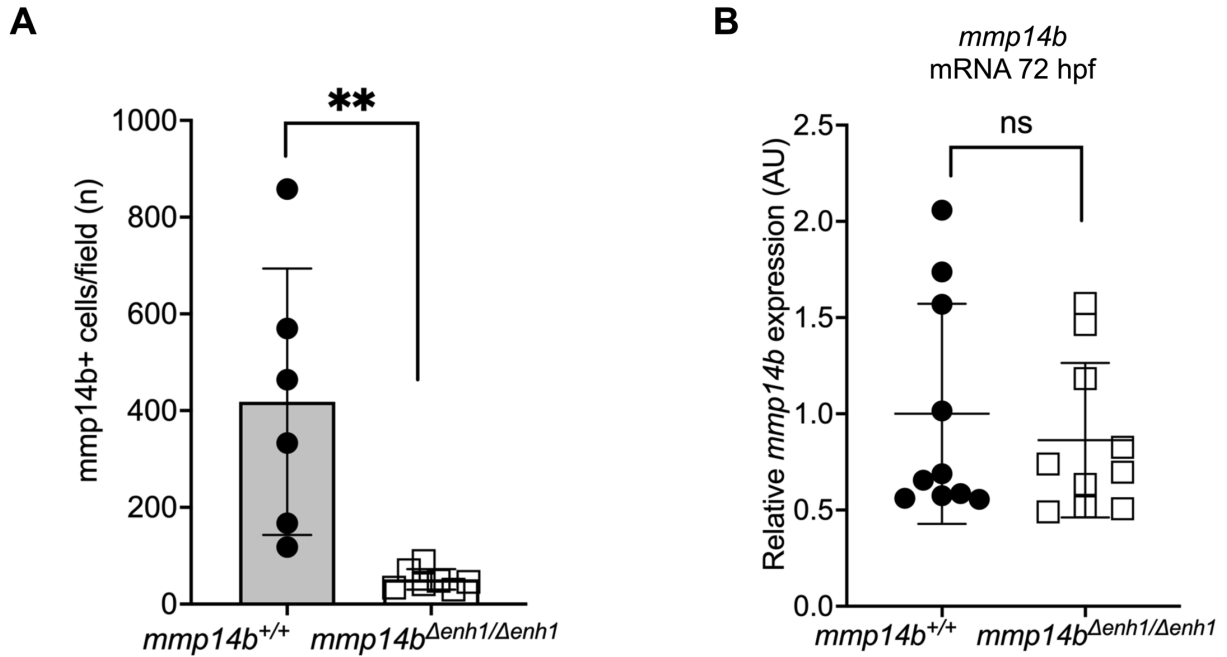


Fig. S7. *mmp14b* expression during development and post-injury in *mmp14b*^{Δenh1/Δenh1} mutant and wild type zebrafish. (A) Quantification of *mmp14b*-positive cells in *mmp14b*^{+/+} and *mmp14b*^{Δenh1/Δenh1} adult zebrafish hearts at 7 dpa. (B) Relative expression of *mmp14b* transcripts in *mmp14b*^{+/+} and *mmp14b*^{Δenh1/Δenh1} zebrafish larvae at 72 hpf. Statistical significance was determined using student's t-test. ns, not significant; **, p<0.01.

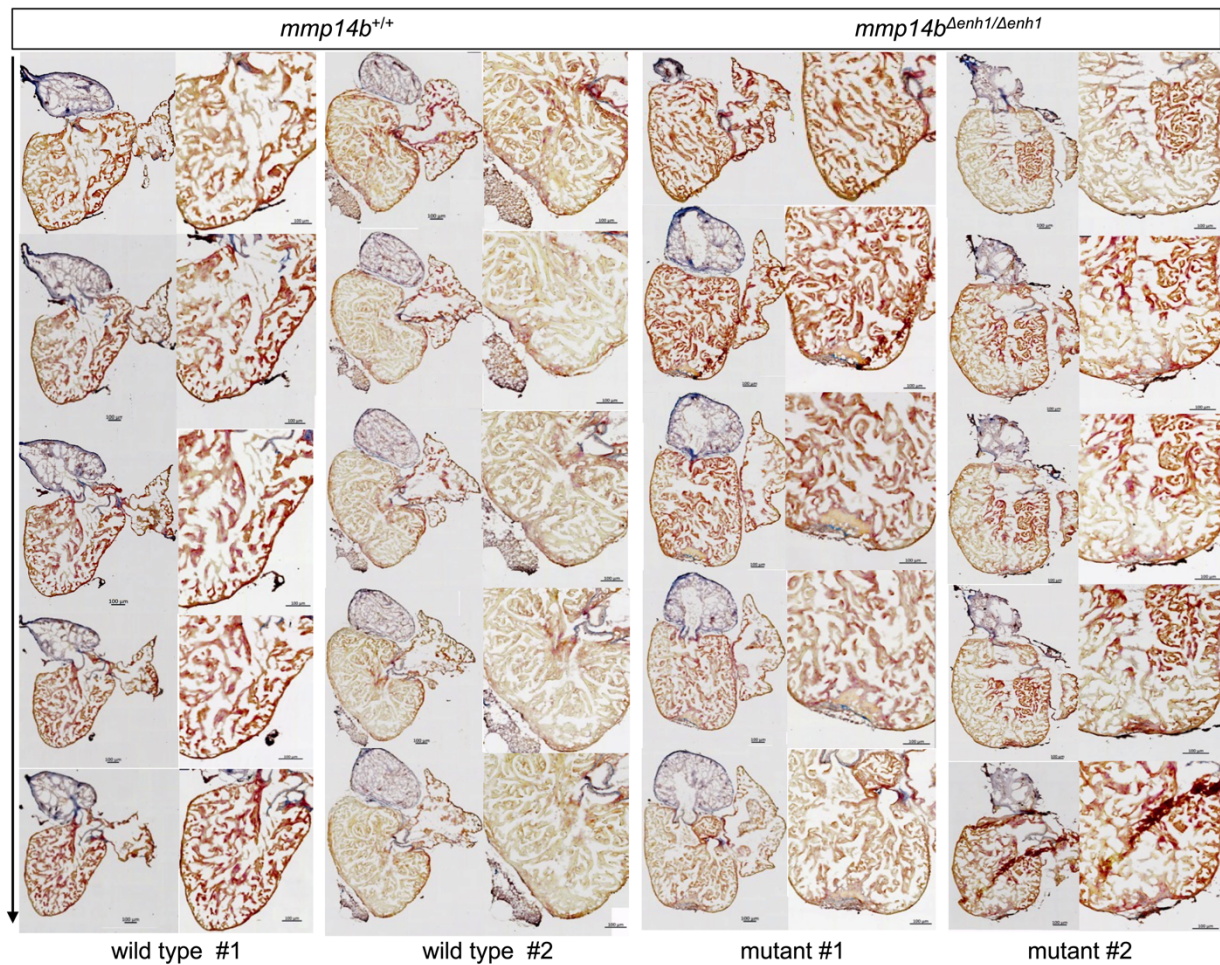


Fig. S8. Scar resolution in *mmp14b*^{Δenh1/Δenh1} mutant and wild type zebrafish. Frontal sections of adult *mmp14b*^{+/+} and *mmp14b*^{Δenh1/Δenh1} zebrafish hearts collected 30 dpa and stained with AFOG to detect muscle (brown), fibrin (red), and collagen (blue). Two wild type *mmp14b*^{+/+} and two mutant *mmp14b*^{Δenh1/Δenh1} with 5 sections per heart shown. Higher magnification images are shown in the right columns for each individual. The *mmp14b*^{+/+} and *mmp14b*^{Δenh1/Δenh1} sections shown in Fig. 5G are distinct sections belonging to the same series as wild type #1 and mutant #1, respectively.

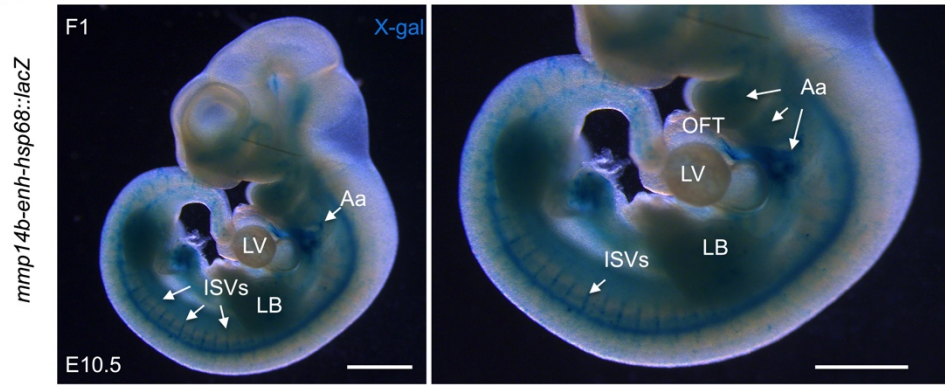
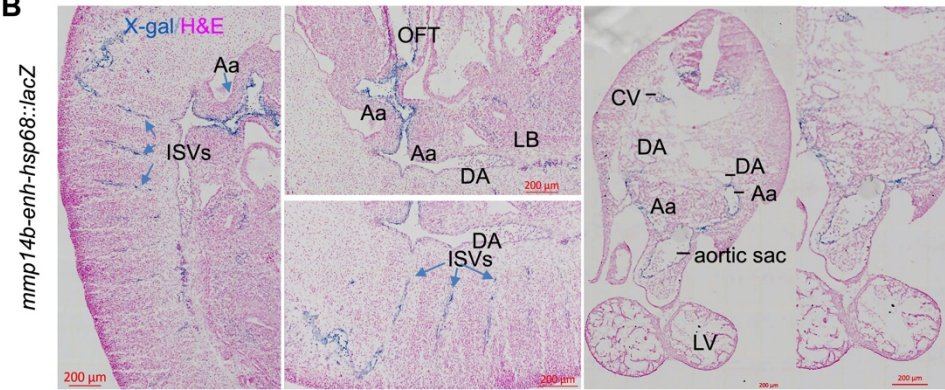
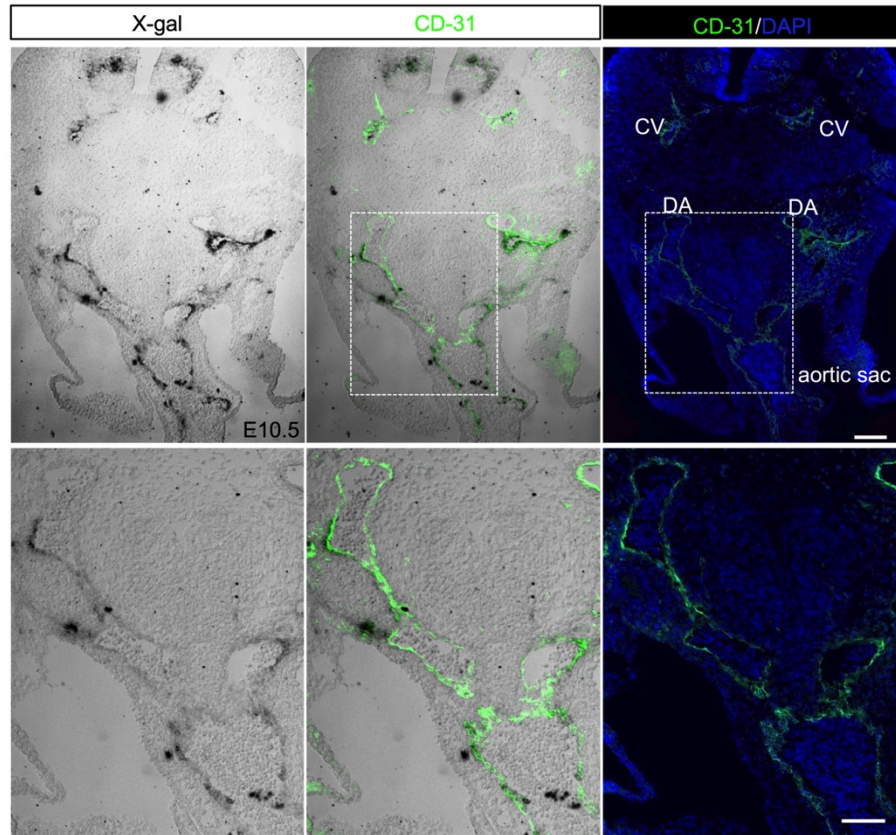
A**B****C**

Fig. S9. Zebrafish *mmp14b-enh* is active in the developing vascular endothelium in mice. Representative images of whole-mount (**A**) and sagittal (**B**, left 3 panels) and transverse (**B**, right two panels and **C**) sections of E10.5 *mmp14b-enh-hsp68::lacZ* embryos stained with X-gal show endothelial-specific activity of zebrafish *mmp14b-enh* in mice. Note the absence of staining in the endocardium, as in the zebrafish. Sections in (**B**) have been counterstained with hematoxylin and eosin (H&E, pink). Sections in (**C**) have been co-immunostained for the endothelial cell marker CD31 (green); overlap with X-gal (middle) and DAPI (right) is shown. The dashed boxes in (**C**, upper row) are shown in magnified views in the lower panels. Note the extensive overlap of β -galactosidase activity (X-gal) and CD31. AA, aortic arches; cardinal vein; DA, dorsal aorta; DLAV; ISV, intersomitic vessels; LB, limb bud; LV, left ventricle; OFT, outflow tract. Scale bars: in (**A**), 1 mm; (**B**), 200 μ m; (**C**), 100 μ m.

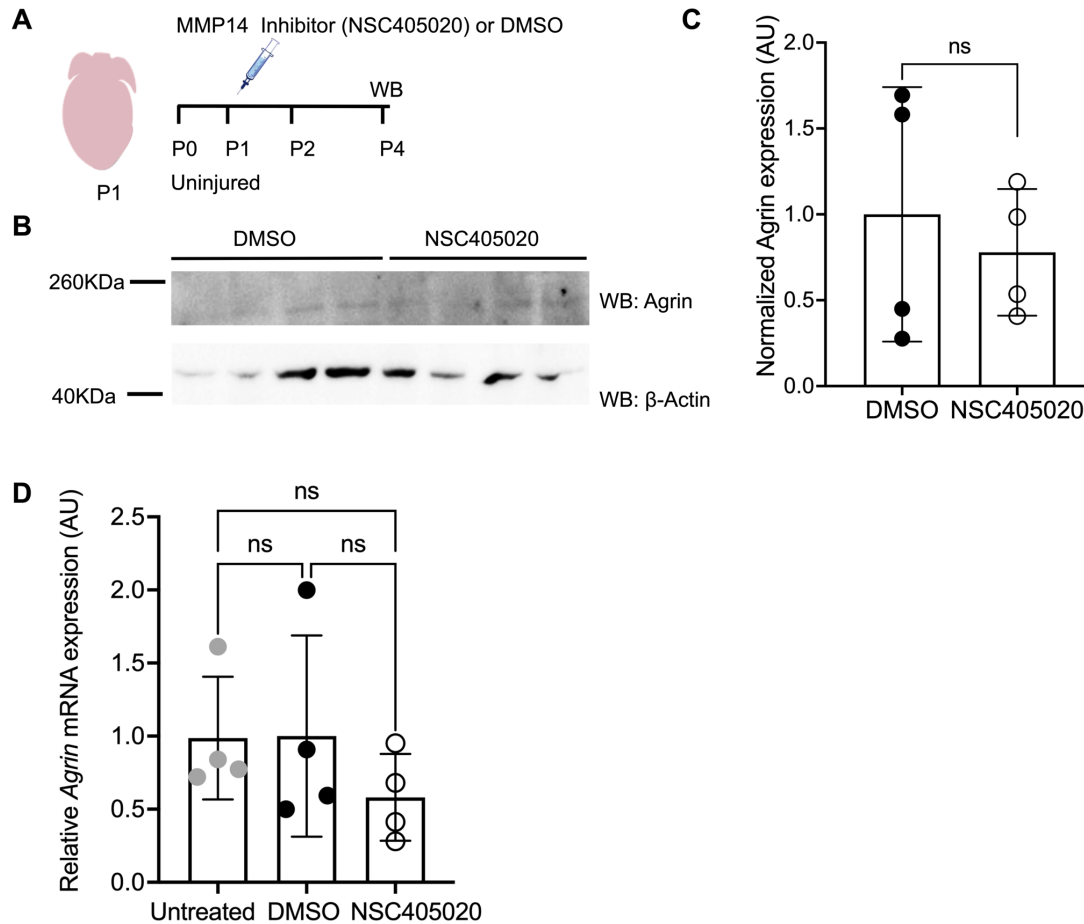


Fig. S10. Basal expression of Agrin in uninjured hearts of neonatal mice treated with NSC405020. (A) Schematic of the experimental design for MMP-14 inhibitor treatment in uninjured neonatal mice. Mice were treated with a single intraperitoneal injection of 20 μ M NSC405020 or DMSO on P1, and hearts were collected on P4 for analysis by western blot (WB). (B) Western blots for Agrin and β -actin from total heart tissue. (C) Quantification of the 260kD isoform of Agrin protein expression (normalized to the expression of β -actin) in uninjured neonatal hearts treated with DMSO or NSC405020. (D) Relative expression of *Agrin* mRNA by qPCR in untreated, DMSO-treated, or NSC405020-treated P4 neonatal hearts. Statistical significance was determined in (C) using student's t-test. Statistical significance in (D) was determined using one-way ANOVA with Tukey's multiple comparisons test. ns, not significant.

Oligonucleotides	Forward Primer	Reverse Primer
Cloning		
<i>mmp14b-enh</i>	5'-ctccatatgggctcttttctctctgttc-3'	5'- aaaacatttctaattgcaggtaaatgactactagttc-3'
<i>mmp14b-enhΔ1</i>	5'- cttcataaggacagaaccgcaggaaatagcccagg-3'	5'-tttctctgttagtctctcttttctaaaatgacatc-3'
<i>mmp14b-enh1[mTEAD]</i>	5'- aaggggggtggtagcttggagaatatagacaaagag-3'	5'- attctccaagctaccacccccttctcatcccactt-3'
Genotyping		
<i>mmp14b-enh</i>	5'-ggatgacatctgtcctcagttac-3'	5'-gcaaagatcttgcgtggtggttc-3'
<i>mmp14b</i>	5'-cttgcgaccttagttggct-3'	5'-agggacctctatgtggttaca-3'
		5'-caaaccagacatgtcaaatgtagta-3'
Cloning-Barcoding		
<i>mmp14b-enh1[Δ1]</i>	5'-ctaaaatgacatcacttttcagcctacaataactt-3'	5'- gtgatgtcattttagtcgagggcccatctggcctg-3'
<i>mmp14b-enh1[Δ2]</i>	5'-cttgcgaccttagttggct-3'	5'- agtattgtaggctgaagagagactaacagagaatc-3'
<i>mmp14b-enh1[Δ3]</i>	5'-tattcttatgcagaattgcatcattcacacca-3'	5'- tctgcataaagaatagtgatgtcattttagaaaag-3'
<i>mmp14b-enh1[Δ4]</i>	5'- gcatcattcacaccaccgcgttctctgccgaa-3'	5'- gggtgtgaatgatgcagtattgtaggctgaaaagt-3'
<i>mmp14b-enh1[Δ5]</i>	5'-gcgttctctgccgaaaacatcaatcccatttc-3'	5'- tcgggcaggaaacgctctgcataaagaatagaaa-3'
<i>mmp14b-enh1[Δ6]</i>	5'-catcaatcccattttccccatctctttgtcta-3'	5'- aaaatgggattgatggggtggaatgatgcaattc-3'
<i>mmp14b-enh1[Δ7]</i>	5'-cccactctttgtctatatttccaacattccac-3'	5'- agacaaagagatgggtcgggcaggaaacgcggtgg-3'
<i>mmp14b-enh1[Δ8]</i>	5'-tttccaacattccacccccttctcatcccac-3'	5'- tggaatgttgagaaaaaatgggattgatgtttc-3'
<i>mmp14b-enh1[Δ9]</i>	5'-ccttctcatcccacttcttctcaaaactctgt-3'	5'- gtgggatgaggaaggagacaaagagatggggg-3'

<i>mmp14b-enh1</i> [Δ10]	5'-cttctcaaactctgtcactacatcaccaaccgt-3'	5'-cagagtttgaggaagtggaatgttgagaatatag-3'
<i>mmp14b-enh1</i> [Δ11]	5'-ctacatcaccaaccgtggcatcatcgacatct-3'	5'-cggttggtgatgtaggtgggatgaggaagggggtg-3'
<i>mmp14b-enh1</i> [Δ12]	5'-gcatcatcgacatctgctctgaagccatgtggt-3'	5'-gatgtcgcgatgatgccagagttgaggaaggaagt-3'
<i>mmp14b-enh1</i> [Δ13]	5'-tctgaagccatgtggtcaaaaaataaaaaatcc-3'	5'-ccacatggcttcagacggttggtgatgtagtgaca-3'
<i>mmp14b-enh1</i> [Δ14]	5'-aaaaataaaaaatccctgggctatttctgcgg-3'	5'-gattttttttttgatgtcgcgatgatccaacg-3'
<i>mmp14b-enh1</i> [Δ15]	5'-gggctatttctgcggttctgtcctatgaaggat-3'	5'-cgcaggaaatagccccacatggcttcagagcaga-3'
<i>mmp14b-enh1</i> [Δ16]	5'-ctgtcctatgaaggatctctcgactctagagggt-3'	5'-tcctcataggacaggatttttttttttacc-3'
<i>mmp14b-enh1</i> [Δ17]	5'-gatctctcgactctagagggtatataatggatcc-3'	5'-tagagtcgagagatccgcaggaaatagcccaggga-3'
EMSA		
TEAD wt	5'-ggggtggaatgttgaga-3'	5'-gggtctccaacattccacc-3'
TEAD muta1	5'-ggggtggttaggttgaga-3'	5'-gggtctccaacctaccacc-3'
TEAD muta2	5'-ggggtggttagcttgaga-3'	5'-gggtctccaagctaccacc-3'
qPCR		
<i>efla</i>	5'-cttctcaggctgactgtgc-3'	5'-ccgctagcattaccctcc-3'
<i>mmp14b</i>	5'-aatggcaaggcgtccagacaaca-3'	5'-ctctcacgttcccggctcgggtca-3'

Table S1. Oligonucleotides used in these studies.

REAGENT or RESOURCE	SOURCE	IDENTIFIER
Antibodies		
Mouse monoclonal MF20	Developmental Studies Hybridoma Bank	DSHB Cat# MF20; RRID: AB_2147781
Mouse monoclonal [PC10] to PCNA	Abcam	Cat# ab201672; RRID: N/A
Rabbit polyclonal anti-Mef2	Santa Cruz Biotech	Cat# sc-313; RRID: AB_631920
Chicken polyclonal anti-GFP	Abcam	Cat# ab13970; RRID: AB_300798
anti-beta Galactosidase	Abcam	Cat#ab9361; RRID: AB_307210
Rabbit polyclonal anti-CD31	Abcam	Cat#ab28364; RRID: AB_726362
Rabbit polyclonal to Agrin (WB)	Abcam	Cat#ab85174; RRID: AB_1860988
Anti-beta-actin clone AC-74 (WB)	Sigma	Cat#A228; RRID: N/A
Goat anti-Rabbit IgG (H+L) Cross-Absorbed Secondary Antibody, Alexa Fluor 488	Thermo Fisher Scientific	Cat# A-11008; RRID: AB_14165
Donkey Anti-Rabbit IgG (H+L) Secondary Alexa Fluor® 647 AffiniPure	Jackson, ImmunoResearch	Cat#711_605_152; RRID: AB_2492288
Goat anti-Mouse IgG (H+L) Cross-Absorbed Secondary Antibody, Alexa Fluor 488	Thermo Fisher Scientific	Cat# A-11029; RRID: AB_2534088
Goat anti-Mouse IgG (H+L) Cross-Absorbed Secondary Antibody, Alexa Fluor 594	Thermo Fisher Scientific	Cat# A-11005; RRID: AB_2534073
Goat anti-chicken IgG (H+L) Cross-Absorbed Secondary Antibody, Alexa Fluor 594	Thermo Fisher Scientific	Cat# A-11042; RRID: AB_2534099
Anti-rabbit IgG, HRP-linked Antibody (WB)	Cell Signaling Technology	Cat# 7074S; RRID: AB_2099233
EasyBlot anti Mouse IgG (HRP)(WB)	GeneTex	Cat# GTX221667-01; RRID: AB_10728926
RNA-scope assays		
RNAscope® Multiplex Fluorescent Reagent Kit v2 - RNAscope® Multiplex Fluorescent Reagent Kit v2. RNA in situ hybridization (ISH)	ACD	Cat#323100
RNAscope® Probe - Dr- <i>mmp14b</i> -C1-Danio rerio matrix metallopeptidase 14b	ACD	Cat#1061661-C1

RNAscope® Negative Control Probe - DapB - Bacillus subtilis strain SMY methylglyoxal synthase (mgsA) gene; dihydrodipicolinate reductase (dapB) gene,	ACD	Cat#310043
RNAscope® Probe - Dr- <i>flilA</i> -C2	ACD	Cat#573351-C2
RNAscope® Probe - egfp-C3	ACD	Cat#400281-C3
TSA PLUS CYANINE	Akoya	Cat# NEL745001KT
TSA PLUS CYANINE 3	Akoya	Cat#NEL744001KT
TSA PLUS FLUORESCHEIN	Akoya	Cat#NEL741001KT
VECTASHIELD Antifade Mounting Medium	Vector Laboratories	Cat# H-1000; RRID: AB_2336789
ProLong Gold Antifade Mountant	Life Technologies	Cat#P36930; RRID:SCR_015961

Table S2. Reagents and antibodies used in these studies.

Data S1. (separate file). Coordinates and neighboring genes of accessible chromatin regions identified in ATAC-seq from endothelial cells from injured versus uninjured zebrafish hearts.